Hindawi Publishing Corporation
Journal of Nanomaterials
Volume 2011, Article ID 919853, 6 pages
doi:10.1155/2011/919853

Research Article

Nanowires of Lead-Free Solder Alloy SnCuAg

F. E. Atalay,[1] D. Avsar,[1] H. Kaya,[1] V. Yagmur,[1] S. Atalay,[1] and T. Seckin[2]

[1] *Department of Physics, Faculty of Science and Art, Inonu University, 44280 Malatya, Turkey*
[2] *Department of Chemistry, Faculty of Science and Art, Inonu University, 44280 Malatya, Turkey*

Correspondence should be addressed to F. E. Atalay, fatalay@inonu.edu.tr

Received 17 December 2010; Accepted 14 March 2011

Academic Editor: Xuedong Bai

Ternary $Sn_{88}Ag_5Cu_7$, $Sn_{93}Ag_4Cu_3$, $Sn_{58}Ag_{18}Cu_{24}$, $Sn_{78}Ag_{16}Cu_6$, $Sn_{90}Ag_4Cu_6$, $Sn_{87}Ag_4Cu_9$ alloy nanowires were produced at various values of deposition potential by dc electrodeposition on highly ordered porous anodic alumina oxide (AAO) templates. During the deposition process some parameters, such as ion content, deposition time, pH, and temperature of the solution, were kept constant. The diameter and length of regular $Sn_{93}Ag_4Cu_3$ nanowires electrodeposited at -1 V were determined by scanning electron microscopy (SEM) to be approximately 200–250 nm and 7-8 μm, respectively. Differential scanning calorimetry (DSC) results indicate that the melting onset temperature of $Sn_{93}Ag_4Cu_3$ nanowires is about 204°C.

1. Introduction

Recently, a number of methods have been developed to fabricate one-dimensional or linear nanostructures, namely, nanotubes and nanowires [1–5]. In the electronic sector, nanowires and nanotubes are attractive nanostructured materials for electronic, optoelectronic, and sensor applications because of their unique properties [1–9]. However, one of the main problems is the nanoscale contact in these nanowires.

As an essential part of electronic circuits, soldering has been made with materials containing Pb until the beginning of 2000. Pb-based materials show good mechanical properties and low melting temperature. Since Pb-based materials have toxic properties and may be harmful for health and the environment, interest in and production of lead-free solder materials have increased enormously. More recently studied lead-free solder materials include $Sn_{96}Ag_{3.5}$ [10, 11], $Sn_{99.5}Cu_{0.7}$ [12], $Sn_{42}Bi_{58}$ [13], $Sn_{48}In_{52}$ [14], SnSb [15], $Sn_{91}Zn_9$ [16, 17], $Sn_{95.5}Ag_{3.8}Cu_{0.7}$ [18], and $Sn_{0.7}Cu_{0.1}Ni$ [19]; the melting temperatures of these materials are 221°C, 217°C, 138°C, 118°C, 235°C, 199°C, 217°C, and 227°C, respectively. Among these solder material alternatives, SnAgCu has begun to be used for making microscale contacts due to its better creep-fatigue resistance and microstructural stability [20].

Technology is developing as a result of the miniaturization of devices as well as the production of nano-sized circuits. Lead-free solder materials have been extensively produced in bulk, powder and thin film forms by different methods over the past decade. Different kind of solder nanowires such as Sn, In, Sn-Ag, Au-Sn, Au-Cu-Sn, Sn-Au-Ni-Au-Sn have been synthesized directly using an electrodeposition method in nanoporous templates [21–23]. However, for nanoscale soldering, SnAgCu material in the form of nanowires is required for production, but until now no studies have been performed on this material. In this work, SnCuAg nanowires have been fabricated by electrodeposition in structured nanoporous Al_2O_3 using various values of the deposition potential.

2. Experimental

A three-electrode cell was used for the electrochemical experiments. The volume of the electrochemical bath was approximately 85 mL. An Ag/AgCl electrode (BAS, 3 M NaCl, and -35 mV versus SCE at 25°C) was used as the reference electrode. Anopore Aluminum Oxide (AAO) membranes, with specified pore diameters of approximately 200 nm and pore length 60 μm, were used as a cathode, with an exposed area of approximately 1 cm^2 for the nanowire synthesis. These membranes were supplied by the Whatman Company. Before the electrodeposition, one side of the AAO templates was coated with Au to a thickness of 5–10 nm and stuck on

Table 1: Bath contents and electrodeposition conditions for production of SnCuAg nanowires.

Chemicals	Concentration
$SnCl_2 \cdot 2H_2O$	40 mM
$CuCl_2 \cdot 2H_20$	1 mM
$Ag(NO_3)_2$	5 mM
$C_6H_{17}N_3O_7$	95 mM
Operating conditions	
Bath pH 4	
Bath temperature = room temperature	
Deposition duration = 180 min	
Deposition potential = −0.75 V–−2 V, versus Ag/AgCl	
Agitation paddle (5 cycles/s)	

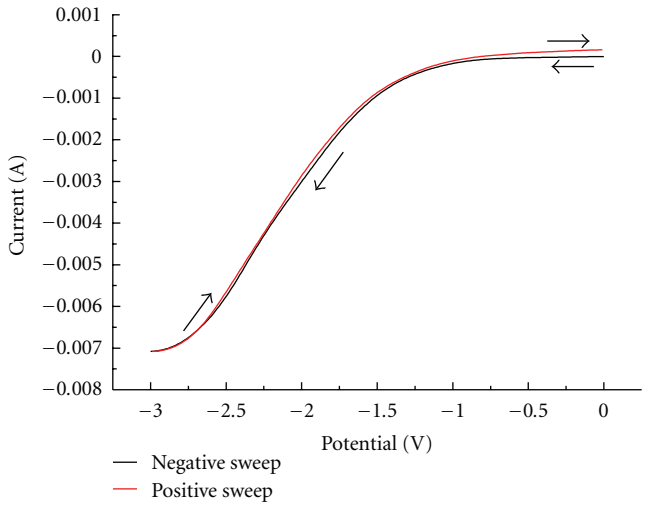

Figure 1: Cyclic voltammograms of Sn-Ag-Cu at 25 mV/s from the bath solution in Table 1 (colour online).

carbon disc on copper plate for electrical contact. A platinum electrode approximately 5 times larger than the cathode was used as an auxiliary electrode. The bath contents are given in Table 1. All solutions were prepared by dissolving reagent-grade chemicals in distilled water. The bath pH was adjusted to 4 by adding 0.1 mM HCl or 0.1 mM NaOH while monitoring with a Jenway 3520 pH meter. The deposition was performed over the potential range −0.75 V to −2 V for 180 minutes to produce the nanowires. The electrodeposition and cyclic voltammetry (CV) for the electroplating of SnAgCu were performed by means of an electrochemical analyzer system, the Iviumstat potentiostat/galvanostat. The scan rate for CV was held constant at 25 mV s^{-1}.

The morphology of the nanoarrays was investigated by scanning electron microscopy (SEM; LEO-EVO-40). The quantitative chemical analyses of the alloys were performed by energy dispersive X-ray (EDX) spectroscopy. X-ray photoelectron spectroscopy (XPS) analyses were made by K-Alpha—Monochromated high-performance XPS spectrometer. X-ray diffraction studies were carried out by using Rigaku-Radb diffractometer equipped with Cu Kα radiation.

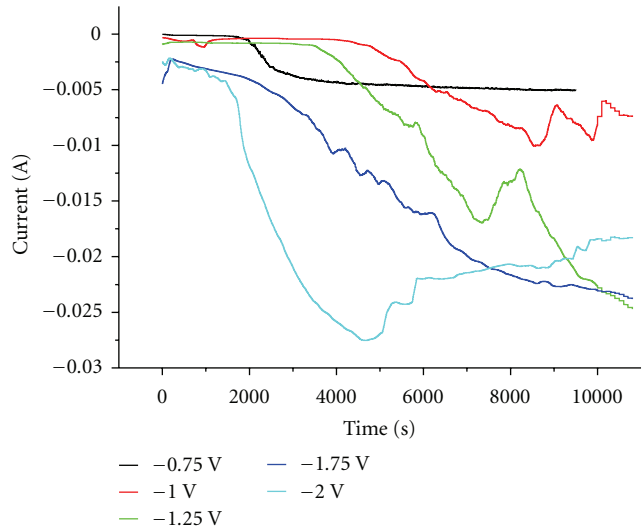

Figure 2: Current transient curves of SnAgCu electrodeposition solution at various deposition potentials for 180 min versus Ag/AgCl.

Differential scanning calorimetry (DSC) was performed in a nitrogen atmosphere with a heating rate of 10°C min^{-1}, using a Shimadzu DSC-60 thermal analyzer.

3. Results and Discussion

A typical cyclic voltammogram for the CV plating of SnAgCu deposition is shown in Figure 1. The CV curve generally shows three reaction regions corresponding to cathodic deposition, no reaction, and anodic oxidation processes, as previously described [24]. In Figure 1, at potentials negative to −0.8 V, on both the positive and negative sweeps, a cathodic current is clearly found, indicating that tin, silver, and copper ions can be deposited into the AAO template. It was observed that neither cathodic deposition nor anodic oxidation occurs when electrode potentials are larger than −0.75 V. The growth rate increases suddenly at potential exceeding −1.25 V.

Figure 2 shows the current behavior as a function of deposition potential during the electrodeposition of nanowires. Electrodeposition curves were obtained in a stirred electrolyte at pH 4. The current versus time plot shows that growth of the nanowires was often not a steady-state process, and it appears that there was significant current oscillation as the voltage was applied to the cathode. At the first stage of the current–time transient curve, the increase in the current when the pores are empty is strongly dependent on the deposition potential. Then the current falls gradually with filling of the pores although there were broad peaks overlapping the decaying current with decreasing deposition potentials. The growth rate increases suddenly at potential exceeding −1.25 V (Figure 2).

It is well known that bath contents and electrochemical deposition parameters have great affects on characteristics of nanowires such as length, appearance. The higher growth

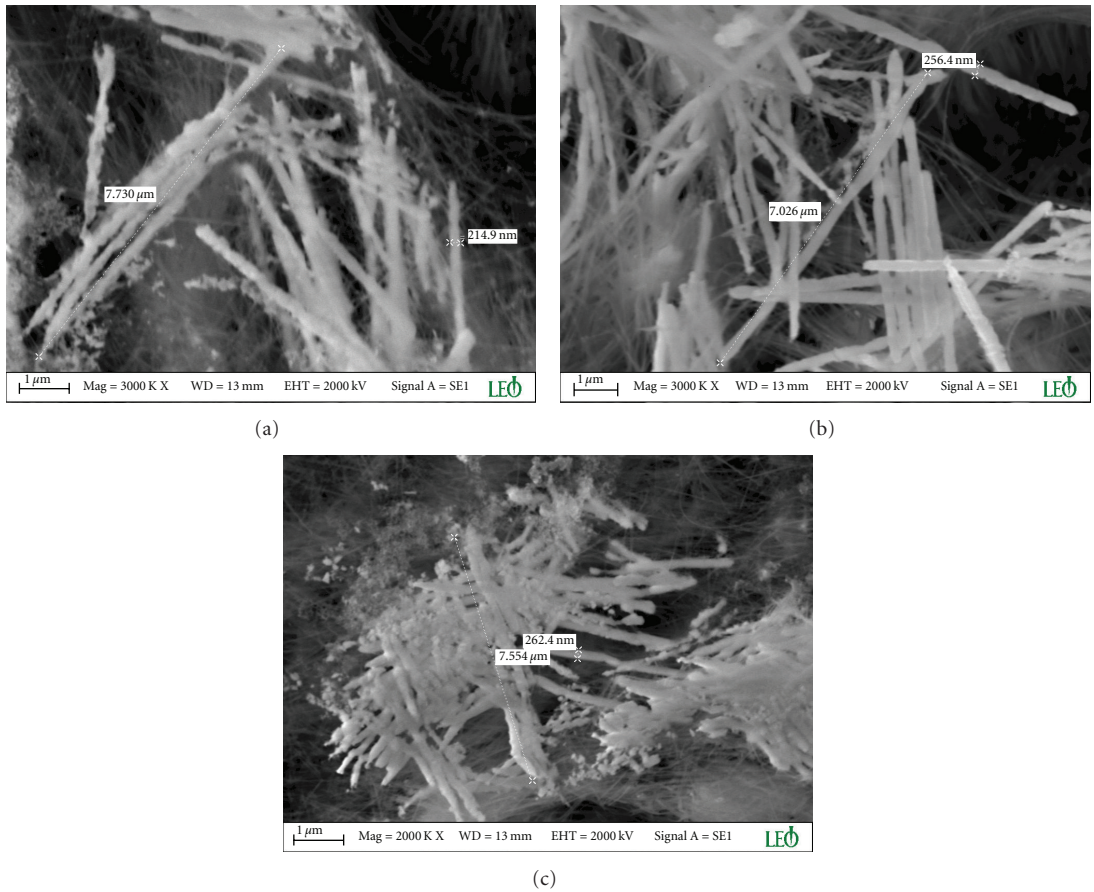

FIGURE 3: SEM images of ordered SnAgCu nanowire arrays electrodeposited at various deposition potentials. (a) −0.75 V, (b) −1 V, and (c) −1.75 V.

rate corresponds to faster metal ions on the tip of the nanowire surface to higher charge density there. Some bubbles are trapped in the nanowire because of higher deposition potentials of −1.5, −1.75, and −2 V. These bubbles electrolyze the water and make the surface rough. The morphology of the SnAgCu nanowires for various values of deposition potential are shown in Figure 3, after complete dissolution of the membrane in 1 M NaOH for 7 minutes. The diameter and length of regular nanowires electrodeposited at −1 V were determined to be approximately 200–250 nm and 8 μm by scanning electron microscopy (SEM) (Figure 3(b)). The nanowires produced at higher potentials of −1.25 V are not uniform along the entire nanowire length.

The average composition of nanowires on the AAO template was evaluated by EDX microanalysis. The unsigned peak rises from the AAO template (Figure 4). It is clearly seen that apparent decrease in intensity of Sn and Ag peaks, if the deposition potential is changed from −1 to −1.25 V. The results indicate that the electrodeposition potential had a marked effect on the Sn, Ag, and Cu content of the SnAgCu deposits (Figure 5). Under the same bath conditions, SnAgCu deposits at −1 V contain more Sn content than those deposited at 0.75 V, −1.25 V, −1.5 V, −1.75 V, −2 V. As can be observed from Figure 5, the compositions of the deposited nanowires were $Sn_{88}Ag_5Cu_7$, $Sn_{93}Ag_4Cu_3$, $Sn_{58}Ag_{18}Cu_{24}$, $Sn_{78}Ag_{16}Cu_6$, $Sn_{90}Ag_4Cu_6$, $Sn_{87}Ag_4Cu_9$ for potentials −0.75 V, −1 V, −1.25 V, −1.5 V, −1.75 V, −2 V, respectively. Significant differences in the morphology of the electrodeposits were observed for different Sn content. When the Sn content is below 93%, SnAgCu nanowires appear in a tree-like pattern, which resembles the branches of the nodes as shown in Figures 3(a) and 3(c).

XRD presented data in Figure 6, mostly in agreement with the recent XRD results for SnAgCu alloy nanoparticles by Jiang et al. [25]. As shown in Figure 6, diffraction pattern of SnAgCu nanowire arrays within AAO demonstrates strong Sn reflections and minor Ag_3Sn and $Cu_{10}Sn_3$ reflections, indicating the successful alloying of Sn-Ag and Cu-Sn during electrodeposition process. No prominent oxide peak was observed from XRD.

Gao et al. [26, 27] reported the size-dependent melting temperature effect of SnAgCu nanoparticles by differential scanning calorimetry (DSC). They observed from the DSC curves of SnAgCu nanostructures that the instability becomes obvious and usually the nanostructures lose stability at lower temperature than their bulk precursors. They have also reported that the depression in melting temperature of SnAgCu nanoparticles can be attributed to the large particle free energy caused by the size effect. Our results agree well with Gao et al. [26, 27]. The melting temperature of

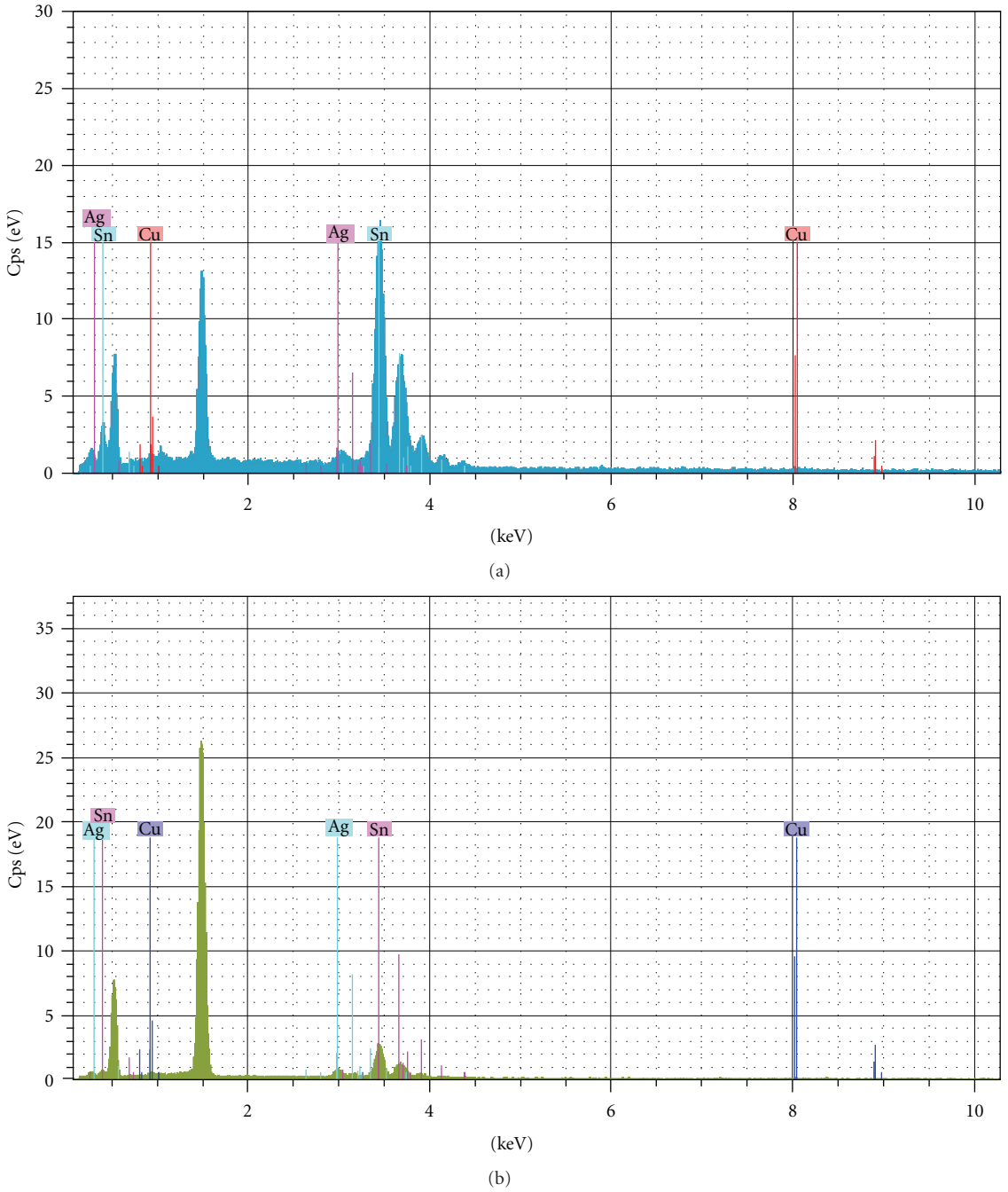

Figure 4: EDX spectrum of SnAgCu nanowire arrays at (a) −1 V and (b) −1.25 V.

the embedded nanowires was determined using a DSC heating rate of 10°C/min (Figure 7). The measured melting temperature was 221.77°C for sample produced at −1 V. The melting onset temperature of $Sn_{93}Ag_4Cu_3$ nanowires is about 204°C. The corresponding latent heat of melting of $Sn_{93}Ag_4Cu_3$ nanowires is about 59.43 J/g.

Figure 8 shows the full XPS spectra of SnAgCu nanowires embedded in AAO template on the surface. The XPS spectrum indicates that surface mainly contains O, C, Sn, Ag, Al, and Cu. XPS is presented in Figure 8, mostly in agreement with the recent XPS results for SnAgCu lead-free solder alloys by Zhang et al. [28]. Existence of C is due to the accumulation of contaminants during exposure to air. Al and most especially O peak is due to from the AAO template.

4. Conclusions

In conclusion, we have successfully, for the first time, fabricated SnAgCu nanowires using template-based electrodeposition. It was shown from SEM micrographs that the nanowires are around 200 nm in diameter and 8 μm in length

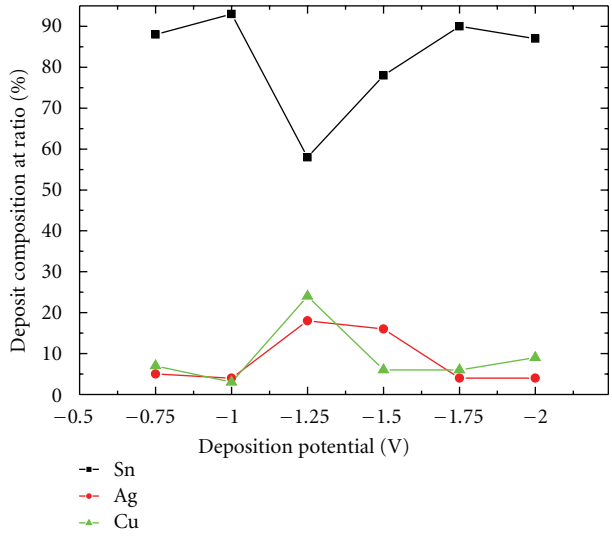

Figure 5: SnAgCu content versus deposition potential obtained by EDX analysis.

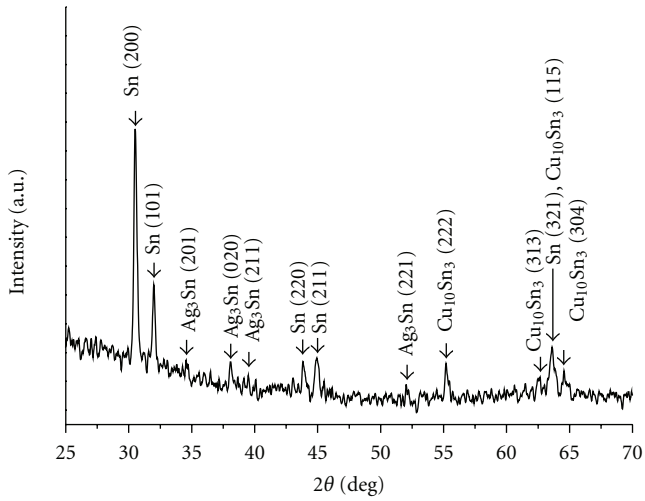

Figure 6: XRD spectrum of SnAgCu nanowire arrays within AAO.

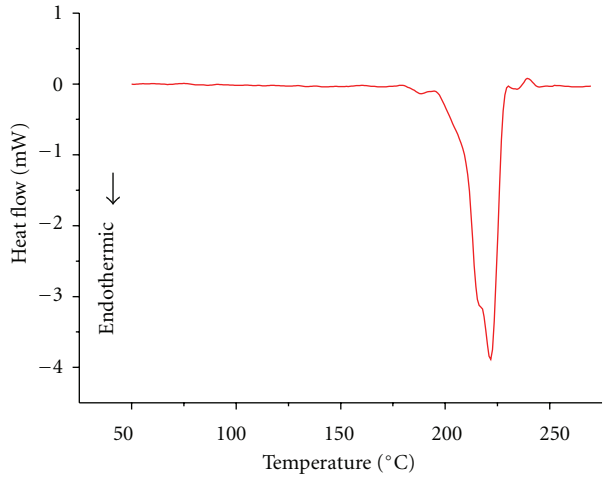

Figure 7: The melting DSC curves of SnAgCu nanowire arrays.

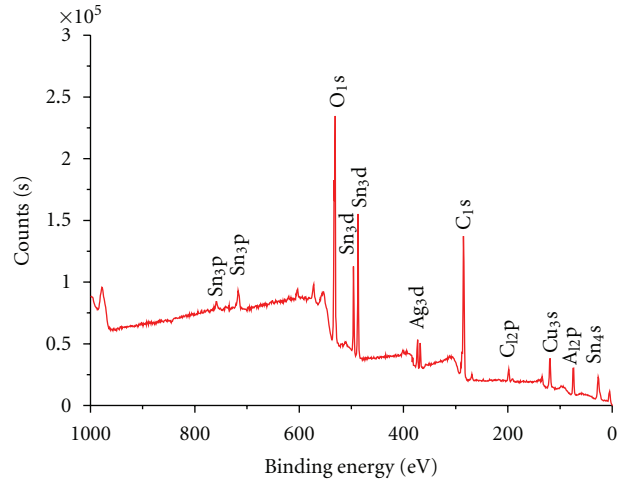

Figure 8: XPS spectrum of SnAgCu nanowire arrays within AAO on the surface.

for a deposition potential of −1 V. SEM and EDX results show that the morphological and composition changes of the nanowires are highly dependent on the deposition potential. It was also observed that the DSC measurement of SnAgCu alloy nanowires shows broad endothermic peak. The melting onset temperature for the nanowires with −1 V deposition potential was about 204°C, which is lower than that of SnAgCu bulk alloy (217–219°C) [29].

Acknowledgment

This work was supported by IUBAPB with Project nos. 2008/62 and 2011/33.

References

[1] B. R. Martin, D. J. Dermody, B. D. Reiss et al., "Orthogonal self-assembly on colloidal gold-platinum nanorods," *Advanced Materials*, vol. 11, no. 12, pp. 1021–1025, 1999.

[2] L. Piraux, J. M. George, J. F. Despres et al., "Giant magnetoresistance in magnetic multilayered nanowires," *Applied Physics Letters*, vol. 65, no. 19, pp. 2484–2486, 1994.

[3] C. N. R. Rao, A. Muler, and A. A. K. Cheetham, *The Chemistry of Nanomaterials*, Wiley-VCH, Weinheim, Germany, 2004.

[4] F. E. Atalay, H. Kaya, S. Atalay, and S. Tari, "Influences of deposition time and pH on magnetic NiFe nanowires fabrication," *Journal of Alloys and Compounds*, vol. 469, no. 1-2, pp. 458–463, 2009.

[5] F. E. Atalay, H. Kaya, V. Yagmur, S. Tari, S. Atalay, and D. Avsar, "The effect of back electrode on the formation of electrodeposited CoNiFe magnetic nanotubes and nanowires," *Applied Surface Science*, vol. 256, no. 8, pp. 2414–2418, 2010.

[6] Y. Xia, P. Yang, Y. Sun et al., "One-dimensional nanostructures: synthesis, characterization, and applications," *Advanced Materials*, vol. 15, no. 5, pp. 353–389, 2003.

[7] S. Dubois, C. Marchai, J. M. Beuken et al., "Perpendicular giant magnetoresistance of NiFe/Cu multilayered nanowires," *Applied Physics Letters*, vol. 70, no. 3, pp. 396–398, 1997.

[8] A. Blondel, J. P. Meier, B. Doudin, and J. P. H. Ansermet, "Giant magnetoresistance of nanowires of multilayers," *Applied Physics Letters*, vol. 65, no. 23, pp. 3019–3021, 1994.

[9] X. Xu and G. Zangari, "Microscopic structure and magnetic behavior of arrays of electrodeposited Ni and Fe nanowires," *Journal of Applied Physics*, vol. 97, no. 10, Article ID 10A306, pp. 1–3, 2005.

[10] Y. Nakamura, Y. Sakakibara, Y. Watanabe, and Y. Amamoto, "Microstructure of solder joints with electronic components in lead-free solders," *Soldering and Surface Mount Technology*, vol. 10, no. 1, pp. 10–12, 1998.

[11] H. Jiang, K. S. Moon, F. Hua, and C. P. Wong, "Synthesis and thermal and wetting properties of tin/silver alloy nanoparticles for low melting point lead-free solders," *Chemistry of Materials*, vol. 19, no. 18, pp. 4482–4485, 2007.

[12] J. C. B. Lee, Y. L. Yao, F. Y. Chiang, P. J. Zheng, C. C. Liao, and Y. S. Chou, "Characterization study of lead-free Sn-Cu plated packages," in *Proceedings of the 52nd Electronic Components and Technology Conference*, pp. 1238–1245, San Diego, Calif, USA, May 2002.

[13] N. M. Poon, C. M.L. Wu, J. K.L. Lai, and Y. C. Chan, "Residual shear strength of Sn-Ag and Sn-Bi lead-free SMT joints after thermal shock," *IEEE Transactions on Advanced Packaging*, vol. 23, no. 4, pp. 708–714, 2000.

[14] D. Suraski and K. Seelig, "The current status of lead-free solder alloys," *IEEE Transactions on Electronics Packaging Manufacturing*, vol. 24, no. 4, pp. 244–248, 2001.

[15] A. Z. Miric and A. Grusd, "Lead-free alloys," *Soldering and Surface Mount Technology*, vol. 10, no. 28, pp. 19–25, 1998.

[16] M. Tadauchi, I. Komatsu, H. Tateishi, and K. Teshima, "Sn-Zn eutectic alloy soldering in a low oxygen atmosphere," in *Proceedings of the 2nd International Symposium on environmentally Conscious Design and Inverse Manufacturing (EcoDesign '01)*, pp. 1055–1059, Tokyo, Japan, 2001.

[17] X. Chen, M. Li, X. X. Ren, A. M. Hu, and D. L. Mao, "Effect of small additions of alloying elements on the properties of Sn-Zn eutectic alloy," *Journal of Electronic Materials*, vol. 35, no. 9, pp. 1734–1739, 2006.

[18] K. Jonnalagadda, M. Pate, and A. Skipor, in *Proceedings of the 8th Intersociety Conference on Thermal and Thermomechanical Phenomena in Electronic Systems*, pp. 915–919, San Diego, Calif, USA, 2002.

[19] K. Sweatman, *Another Chance for Tin-Copper as a Lead-Free Solder*, Apex Special Issue, 2005.

[20] M. Erinc, P. J. G. Schreurs, and M. G. D. Geers, "Integrated numerical-experimental analysis of interfacial fatigue fracture in SnAgCu solder joints," *International Journal of Solids and Structures*, vol. 44, no. 17, pp. 5680–5694, 2007.

[21] F. Gao, S. Mukherjee, Q. Cui, and Z. Gu, "Synthesis, characterization, and thermal properties of nanoscale lead-free solders on multisegmented metal nanowires," *Journal of Physical Chemistry C*, vol. 113, no. 22, pp. 9546–9552, 2009.

[22] Z. Gu, H. Ye, D. Smirnova, D. Small, and D. H. Gracias, "Reflow and electrical characteristics of nanoscale solder," *Small*, vol. 2, no. 2, pp. 225–229, 2006.

[23] C. C. Chen, Y. Bisrat, Z. P. Luo, R. E. Schaak, C. G. Chao, and D. C. Lagoudas, "Fabrication of single-crystal tin nanowires by hydraulic pressure injection," *Nanotechnology*, vol. 17, no. 2, pp. 367–374, 2006.

[24] A. Bai and C. C. Hu, "Effects of electroplating variables on the composition and morphology of nickel-cobalt deposits plated through means of cyclic voltammetry," *Electrochimica Acta*, vol. 47, no. 21, pp. 3447–3456, 2002.

[25] H. Jiang, K. Moon, and P. Wong, "Tin/silver/copper alloy nanoparticle pastes for low temperature lead-free interconnect applications," in *Proceedings of the 58th Electronic Components and Technology Conference (ECTC '08)*, vol. 4, pp. 1400–1404, Lake Buena Vista, FL, USA, May 2008.

[26] Y. Gao, C. Zou, B. Yang et al., "Nanoparticles of SnAgCu lead-free solder alloy with an equivalent melting temperature of SnPb solder alloy," *Journal of Alloys and Compounds*, vol. 484, no. 1-2, pp. 777–781, 2009.

[27] C. D. Zou, YU. L. Gao, B. Yang et al., "Nanoparticles of the lead-free solder alloy Sn-3.0Ag-0.5Cu with large melting temperature depression," *Journal of Electronic Materials*, vol. 38, no. 2, pp. 351–355, 2009.

[28] S. Zhang, Y. Zhang, and H. Wang, "Effect of oxide thickness of solder powders on the coalescence of SnAgCu lead-free solder pastes," *Journal of Alloys and Compounds*, vol. 487, no. 1-2, pp. 682–686, 2009.

[29] I. E. Anderson, J. C. Foley, B. A. Cook, J. Harringa, R. L. Terpstra, and O. Unal, "Alloying effects in near-eutectic Sn-Ag-Cu solder alloys for improved microstructural stability," *Journal of Electronic Materials*, vol. 30, no. 9, pp. 1050–1059, 2001.